EUROPEAN COMMISSION

Community research

EURATOM

Long-term Performance of Engineered Barrier Systems

PEBS

Long-term Performance of Engineered Barrier Systems

PEBS

DELIVERABLE (D-N^{O}:DB-2.4)

China-Mock-up status Annual Report

Authors:

Yuemiao Liu, Ju Wang, Shengfei Cao, Liang Chen

Date of issue of this report:01/03/2014

Start date of project: 01/03/10 Duration: 48 Months

Seventh Euratom Framework Programme for Nuclear Research & Training Activities		
Dissemination Level		
PU	Public	PU
RE	Restricted to a group specified by the partners of the PEBS project	
CO	Confidential, only for partners of the PEBS project	

中核集团核工业北京地质研究院

CNNC Beijing Research Institute of Uranium Geology

CONTENTS

ABSTRACT

According to the preliminary concept of the high level radioactive waste (HLW) repository in China, a large-scale mock-up facility, named China-Mock-up was constructed in the laboratory of BRIUG, a heater, which substitutes a container of radioactive waste, is placed inside the compacted GMZ-Na-bentonite blocks and pellets. Water inflow through the barrier from its outer surface is to simulate the intake of groundwater. The current experimental data of the facility is reported and analyzed in the report. The real-time data acquisition and monitoring system has recorded all the measurement data from 1st April 2011 to 11th December 2013. It is revealed that the saturation process of the compacted bentonite is strongly influenced by the competitive mechanism between the drying effect induced by the high temperature and the wetting effect by the water penetration from outer boundary. For this reason, the desiccation phenomenon is observed in the zone close to the heater. The displacement of the heater and the stress evolution is also mentioned.

In the report, a constitutive model is proposed to tackle the principal THM coupling behavior of GMZ bentonite. With the proposed model, numerical simulations of the China-Mock-up test are carried out by using the code of LAGAMINE. A qualitative analysis of the predictive results is carried out, including the variation of temperature, saturation degree, suction and swelling pressure of the compacted bentonite. It is suggested that the proposed model is capable to reproduce the principal physico-mechanical behavior of GMZ bentonite.

KEYWORDS: High-level radioactive waste (HLW), geological repository, bentonite, lab testing, numerical modeling, thermo-hydro-mechanical-chemical (THMC)

1. Background

Geological repositories are generally designed on the basis of a multiple barrier system concept, which is mainly composed by engineered and natural barriers. In the life cycle of the high-level radioactive waste (HLW) disposal project, the buffer/backfill will be subjected to temperature increase due to heat emitted by the waste and hydration from water coming from the adjacent rocks (Gens et al, 2010). The buffer/backfill material is designed to stabilize the repository excavations and the coupled thermo-hydro-mechanical-chemical (THMC) conditions, and to provide low permeability and long-term retardation (Wang, 2010). A bentonite-based material is often proposed or considered as a possible buffer/backfill material for the isolation of the HLW.

To understand the complex behaviors of the buffer/backfill material located in the coupled THMC environment, in recent years, there has been an increasing interest internationally in the construction of large-scale mock-up experimental facilities in the laboratory and in situ such as the Long Term Experiment of Buffer Material (LOT) series at the Äspö HRL in Sweden (Karnland et al, 2000), FEBEX experiment in Spain (Lloret & Villar, 2007), OPHELIE and PRACLAY heater experiments in Belgium (Li et al, 2006, 2010, Romero & Li, 2010) and Mock-Up-CZ experiment in Czech Republic (Pacovsky et al, 2007) etc. The experimental results and achievements obtained from these large-scale experiments provide important references on investigating the behaviors of bentonite under simulative nuclear radioactive waste repository conditions.

At the present stage, the Gaomiaozi (GMZ) bentonite is considered as the candidate buffer and backfill material for the Chinese repository. Lots of basic experimental studies have been conducted and favorable results have been achieved (Liu et al., 2003; Liu & Cai, 2007a; Ye et al. 2009a). In order to further study the behavior of the GMZ-Na-bentonite under relevant repository conditions, a mock-up facility, named China-Mock-up, was proposed based on a preliminary concept of HLW repository in China (Liu et al., 2011). The experiment is intended to evaluate THMC processes taking place in the compacted bentonite-buffer during the early phase of HLW disposal and to provide a reliable database for numerical modeling and further investigations.

In order to predict the long-term behavior of GMZ-Na-bentonite under physico-

mechanical coupling condition, an essential objective of the China-Mock-up test consists to establish a numerical approach. In this regard, a constitutive model is proposed to tackle the physical-mechanical behavior of GMZ-Na-bentonite (Chen et al, 2012). In the model, the following physical phenomena are taken into account: the transport of liquid (advection) and heat (convection and conduction), the vapor diffusion, the evaporation and condensation phenomena of water. The constitutive model of Alonso-Gens (1990) is used to reproduce the fundamental mechanical features of the GMZ bentonite in partially saturated condition. In order to validate the proposed model, a preliminary numerical simulation of the China-Mock-up test is carried out by the program LAGAMINE developed at Liege University (Charlier, 1987). The qualitative analysis of the predictive result is realized.

The overall approach is based on performing experiments according to the needs for additional studies on key processes during the early EBS evolution. The study will make use to the extent possible of on going experiments being conducted in the laboratory of Beijing Research Institute of Uranium Geology (BRIUG).

2. The T-H-M-C China-Mock-Up experiment

The China-Mock-up is mainly made up of eight components, namely compacted bentonite blocks, steel tank, heater and corresponding temperature control system, hydration system, sensors, gas measurement and collection system, real-time data acquisition and monitoring system (Fig. 1).

It is assumed that the duration of the China-Mock-up experiment will not be shorter than 4 years. Then, after a cooling period, the experiment will be dismantled and all the available results will be collected and evaluated.

The China-Mock-up experiment was assembled completely on 10th September 2010. The real-time data acquisition and monitoring system has recorded all the measurement data from1st April 2011. And the heater was switched on to reach a low temperature at 30°C from 1st April 2011 until 8th July 2011. The T-H-M-C experiment was commenced on 8th July 2011, then the power rises at 1°C/d to reach a maximum temperature at 90°C. In order to avoid potential damage to the sensors, the hydration was initially controlled by a water injection rate which was increased gradually from 400g/day to 1500 g/day in the first stage, and the injection was controlled by a constant pressure at 0.2Mpa from 25th August 2013.

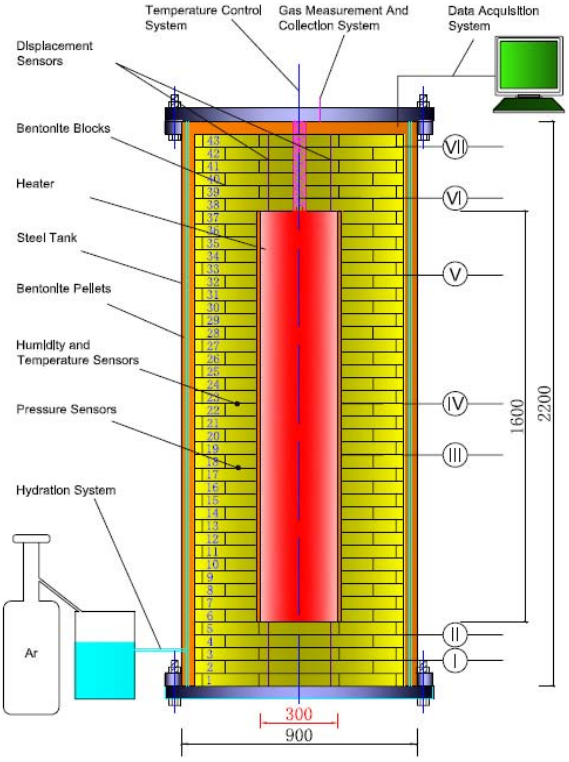

Figure 1 Sketch of the China-Mock-up facility (unit: mm).

3. Experiment results of China-Mock-up

The China-Mock-up is equipped with 10 different types of sensors to monitor the comprehensive performances of GMZ Na-bentonite under coupled THMC conditions. The sensors placed in the bentonite have provided reasonable and consistent recordings, and continue to do so in the next operation phase of the experiment. The experimental results of characterization performed concerning coupled T-H-M properties are reported and analyzed in this chapter. The time variation of the water consuming, relative humidity, temperature, and swelling pressured of the compacted bentonite are studied. The real-time data acquisition and monitoring system has recorded all the measurement data from 1st April 2011 to 11th December 2013.

3.1 Mock-up operation

The China-Mock-up experiment was assembled completely on 10th September 2010. After

a pre-operational phase, the real-time data acquisition and monitoring system has recorded all the measurement data from1st April 2011, and the data identified as “day 0” on the time scale.

3.1.1 Heating

The heater was switched on to reach a low temperature at 30°C from 1st April 2011 until 8th July 2011. The T-H-M-C experiment was commenced on 8th July 2011, then the power rises at 1°C/d to reach a maximum temperature at 90°C. Finally, the heating system was switched to the constant temperature control model automatically at 90°C. The heating phase with the time is illustrated in Fig. 2.

3.1.2 Hydration

The hydration process was carried out with Beishan groundwater. In order to avoid potential damage to the sensors by a sudden saturation process, the hydration was initially controlled by a water injection rate which was increased gradually from 400g/day to 1500 g/day in the first stage, and the injection was controlled by a constant pressure at 0.2Mpa from 25th August 2013. The water consuming with the time is illustrated in Fig. 2. To mentioned here, the water injection was preformed artificially every day in the first stage, and the platforms illustrated in Fig. 2 indicates no water supply during the corresponding period of time.

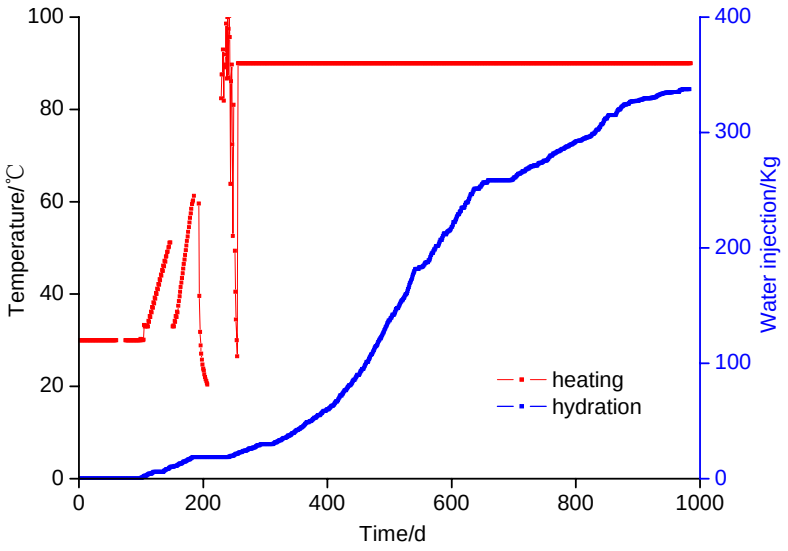

Figure 2 Mock-up operation.

3.2 Temperature

The temperature variation with time in different sections of the facility is illustrated in Fig. 3-9. As the beginning of the test, the temperature is increased globally with time, especially for the sensors close to the heater, the temperature has decreased distance from the heater. Due to the interrupt of electricity power, some fluctuation can be observed. It is noticed that the change of seasons has a significant effect on temperature, but unfortunately some of the sensors are out of work because of the harsh environment.

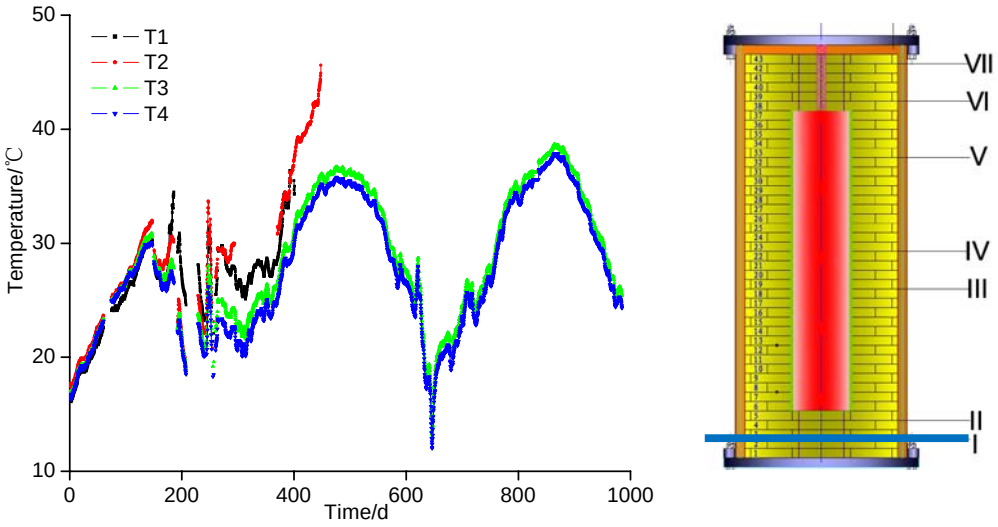

Figure 3 Temperature variation with time at section I.

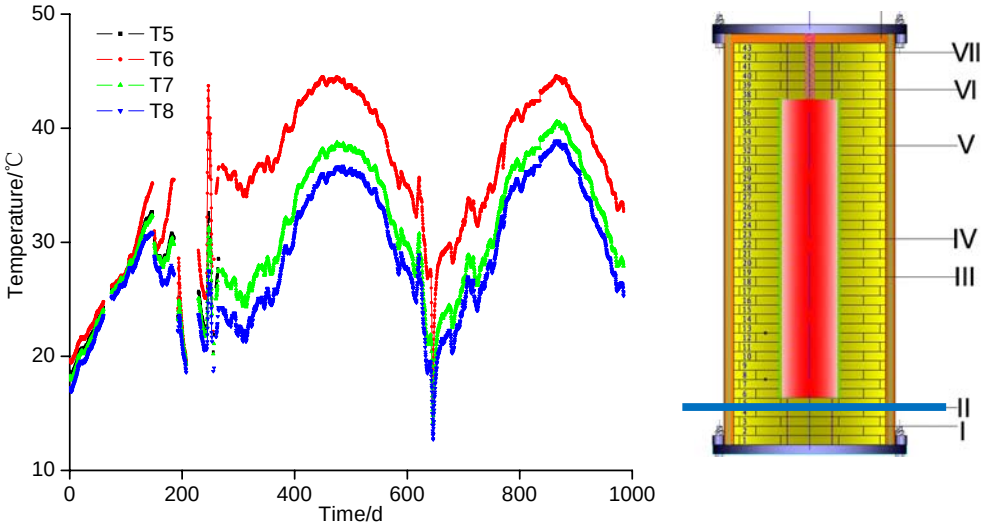

Figure 4 Temperature variation with time at section II

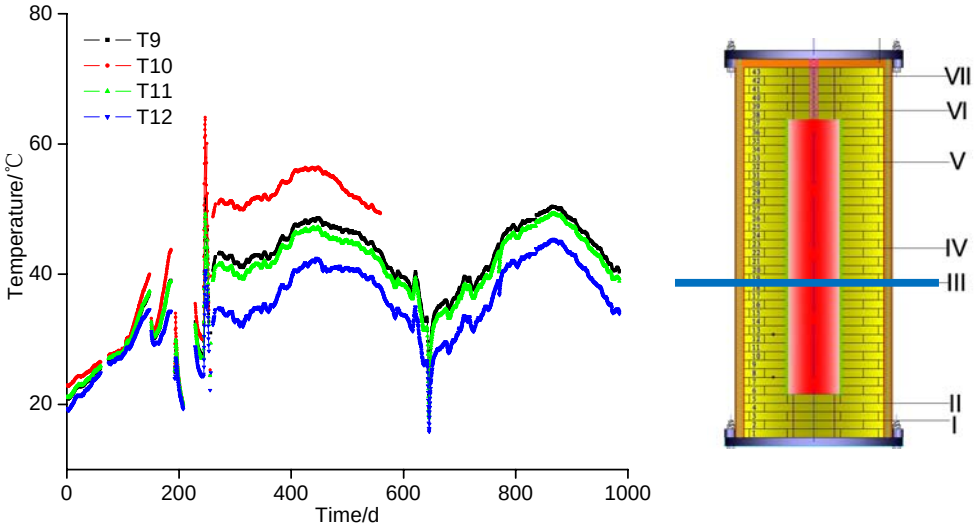

Figure 5 Temperature variation with time at section III.

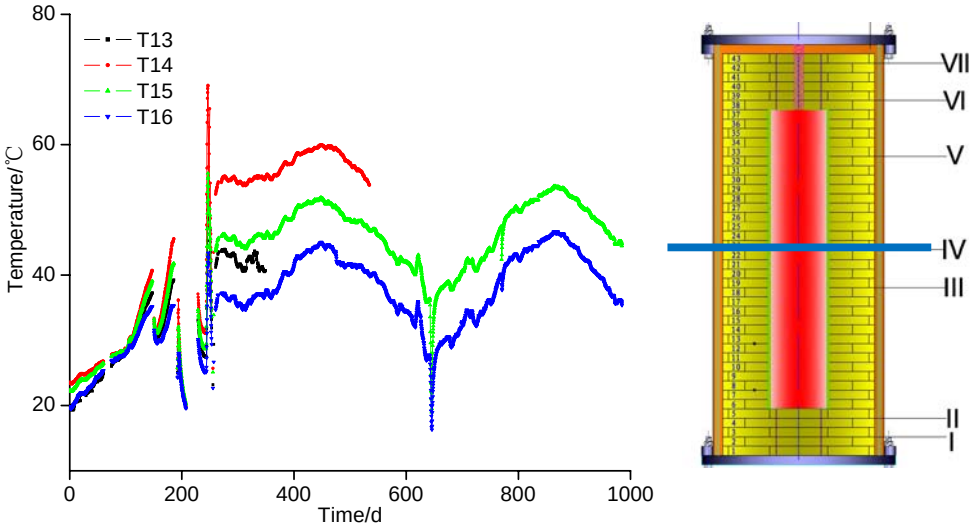

Figure 6 Temperature variation with time at section IV.

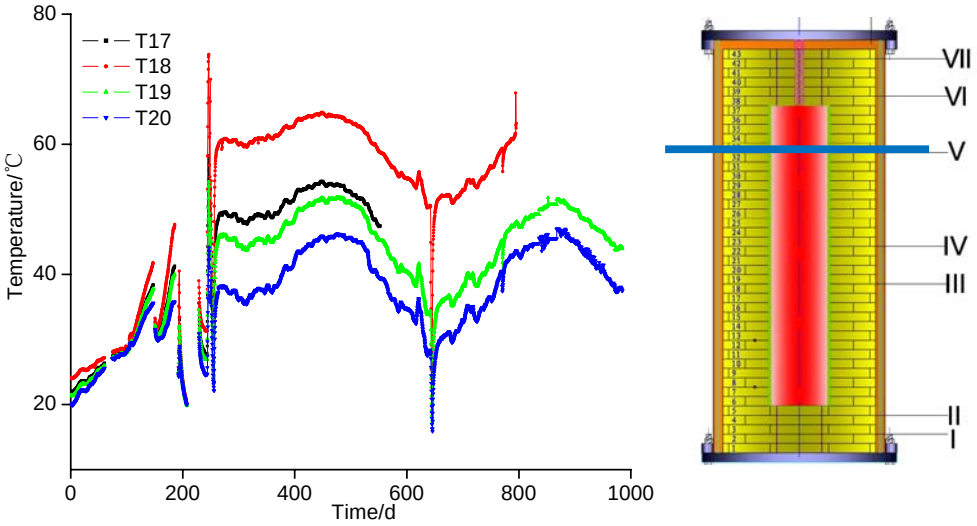

Figure 7 Temperature variation with time at section V.

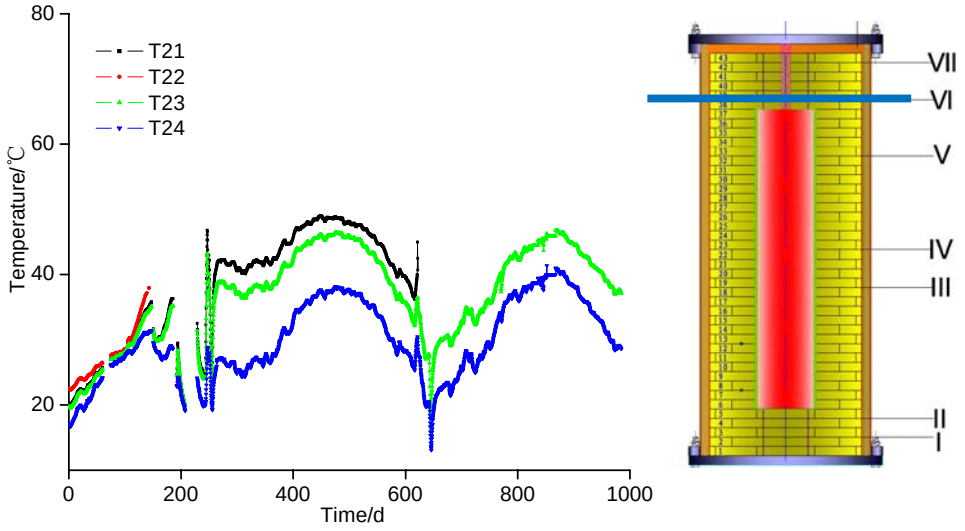

Figure 8 Temperature variation with time at section VI.

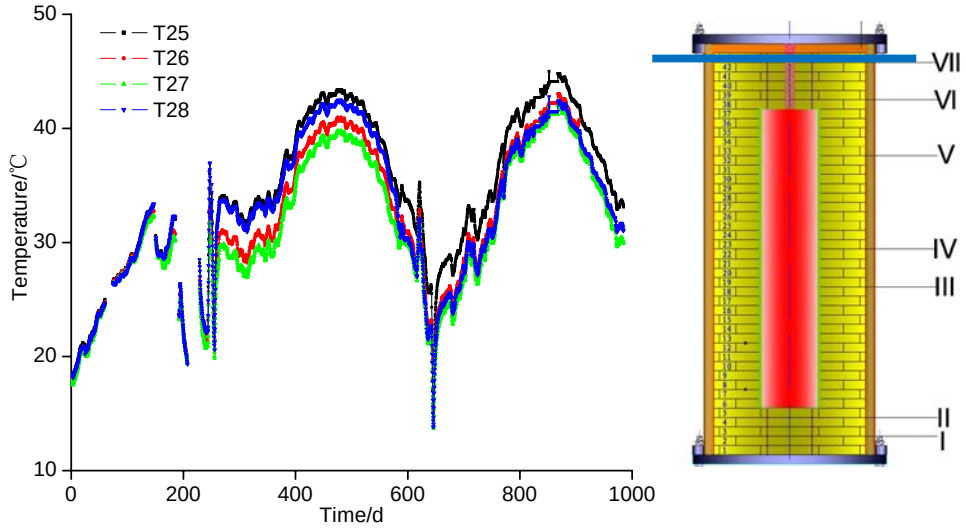

Figure 9 Temperature variation with time at section VII.

3.3 Relative humidity

Fig. 10 and Fig. 11 present the relative humidity variation with time at the bottom of the mock-up facility. As illustrated in the figures, the compacted bentonite is progressively saturated with time in section I and II, and the distance to the outer boundary has a significant influence on the saturation velocity. In the area close to the outer boundary (H3 and H6), the compacted bentonite is almost saturated after 200 days. Due to the extremely low permeability of compacted bentonite, the variation of relative humidity is limited in the central part of the facility. However, the bentonite in section I and II is totally saturated with the increase of the injection water after 600 days.

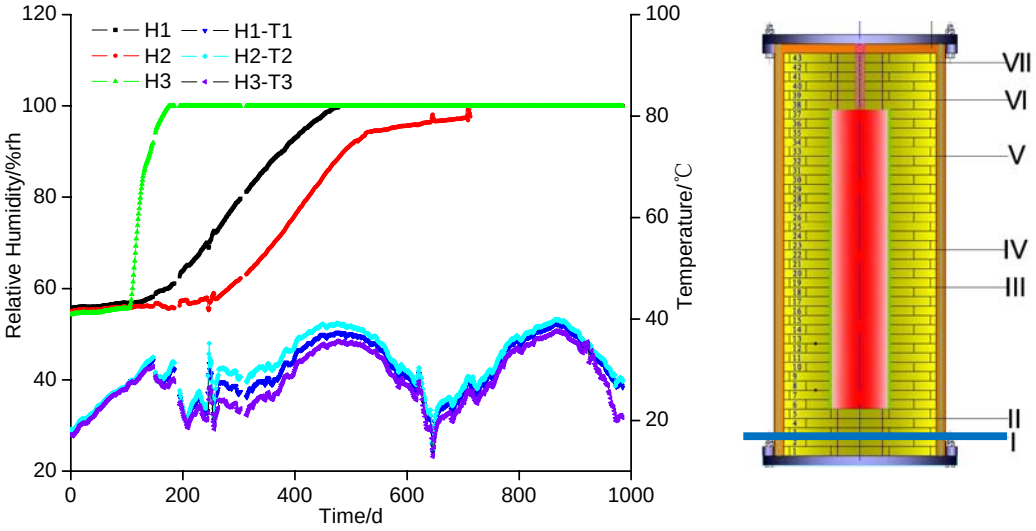

Figure 10 Relative humidity distribution at section I.

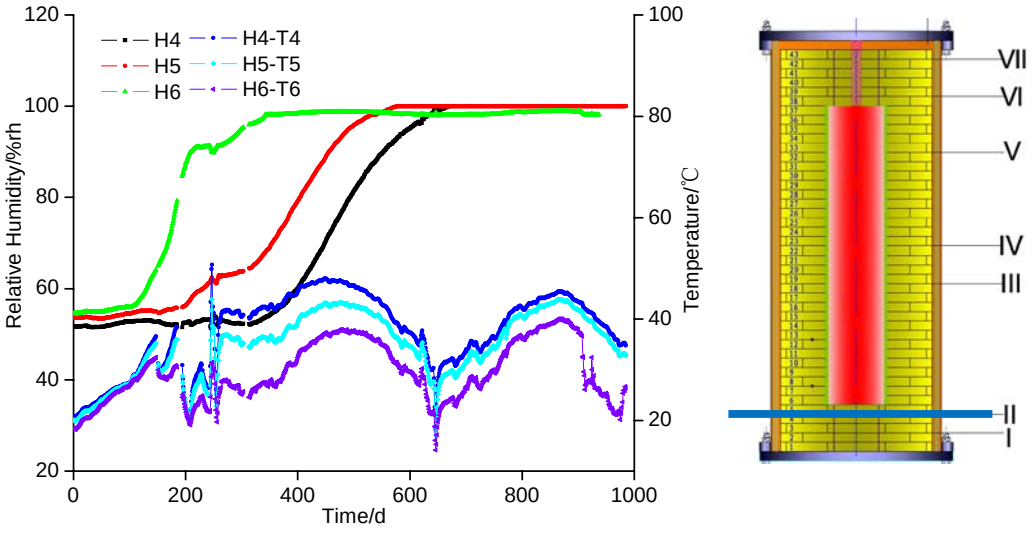

Figure 11 Relative humidity distribution at section II.

Fig. 12-14 presents the variation of relative humidity with time in the sections III-V. It can be noticed that, the variation of relative humility in this area is much more complex. In the zone close to the heater, the decrease of relative humidity can be observed. This phenomenon can be attributed to the competitive mechanism between the saturation process induced by the water penetration and the drying effect by the high temperature of the electrical heater. The desaturation phenomenon indicates that, due to the low permeability of the compacted

bentonite, the drying effect is dominant at the beginning in the zone close to the heater. Then with the increase of the injection water, the saturation process is dominant after 500 days, and the humility is increased gradually.

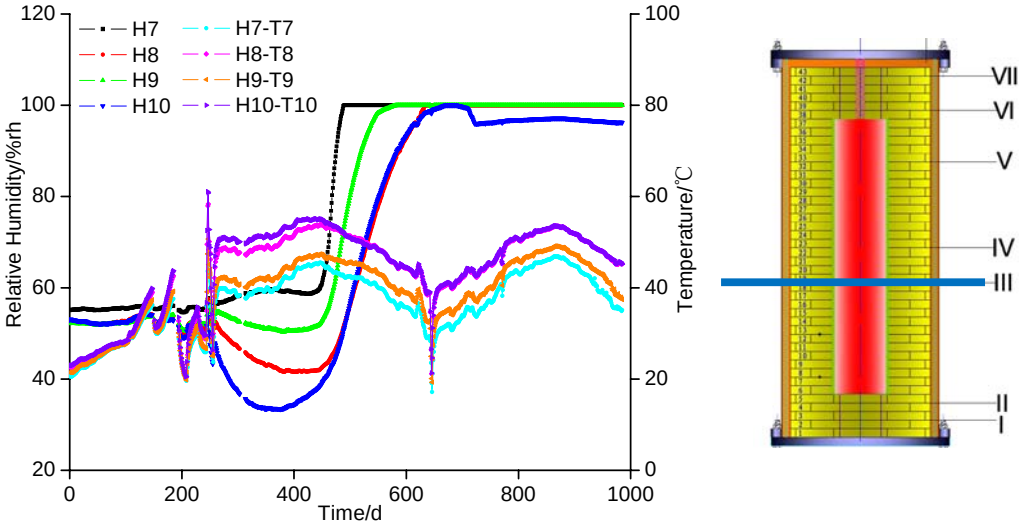

Figure 12 Relative humidity distribution at section III.

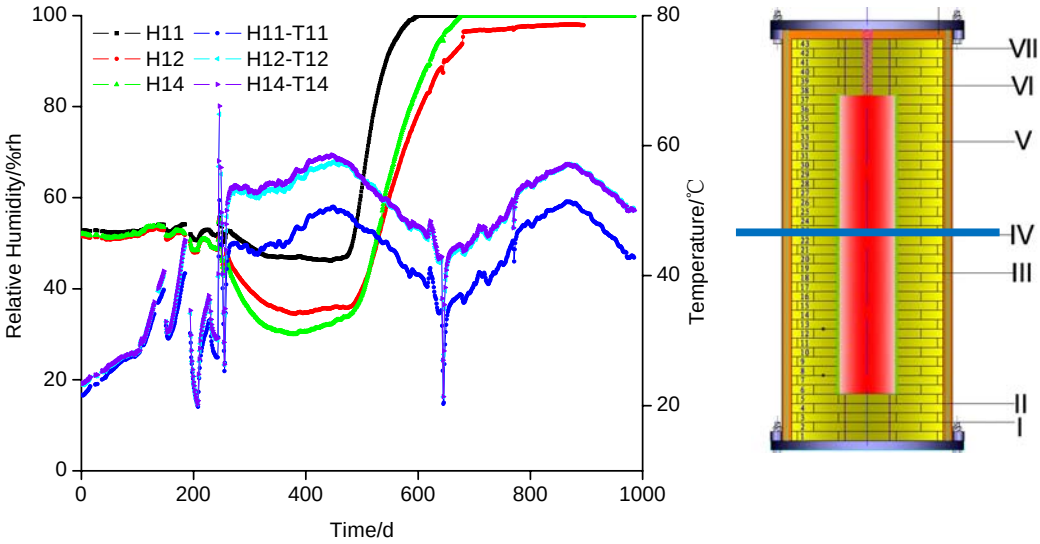

Figure 13 Relative humidity distribution at section IV.

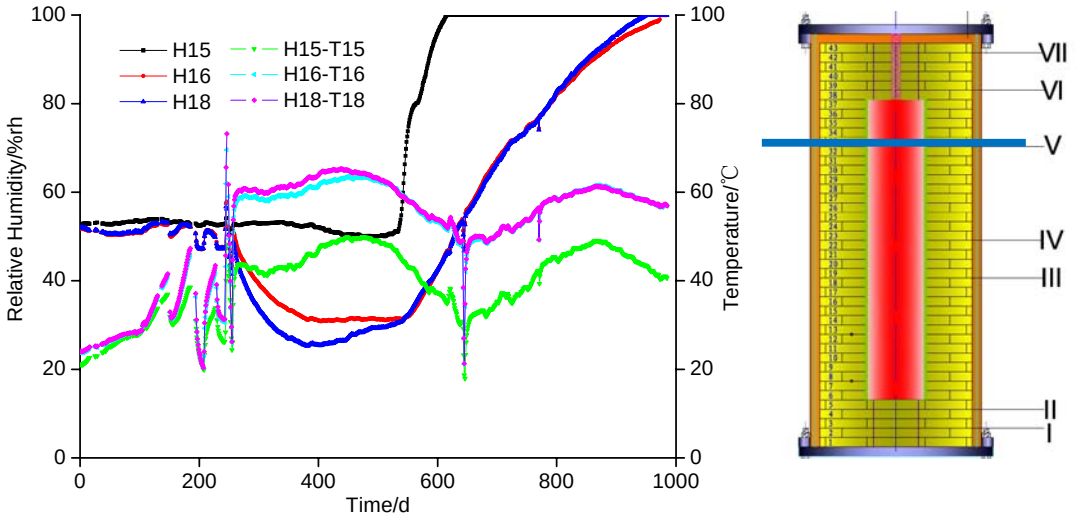

Figure 14 Variation of relative humidity at section V.

The variation of relative humidity with time on the top of the China-mock-up facility is illustrated in Fig. 15-16. Thanks to the longer distance to the heater, it can be noticed that the desiccation induced by the high temperature is less evident in this area. However, the desaturation phenomenon is still noticed in the central part of the section with the increase of temperature in this area. In addition, the relative humidity is sensitive to the fluctuation of the temperature.

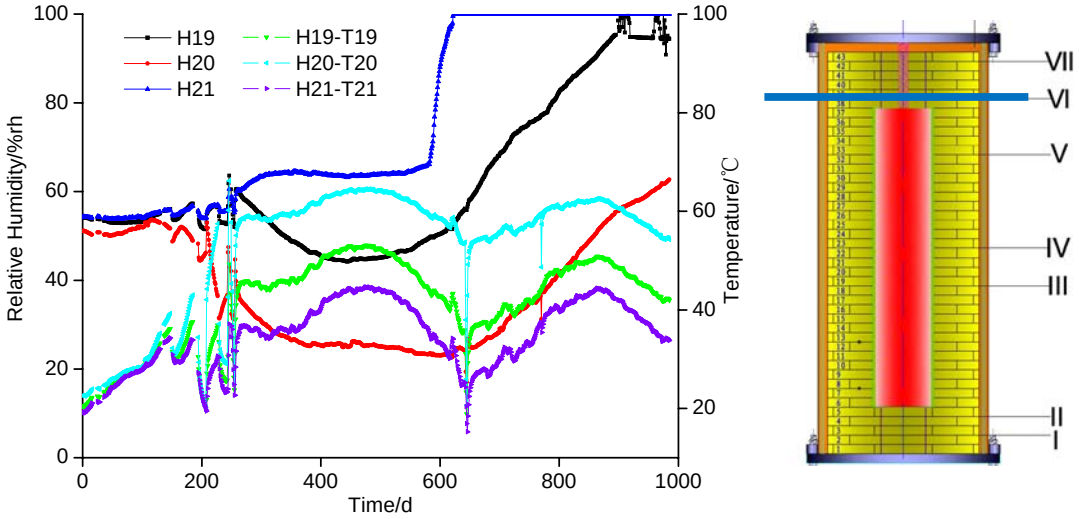

Figure 15 Variation of relative humidity with time at section VI.

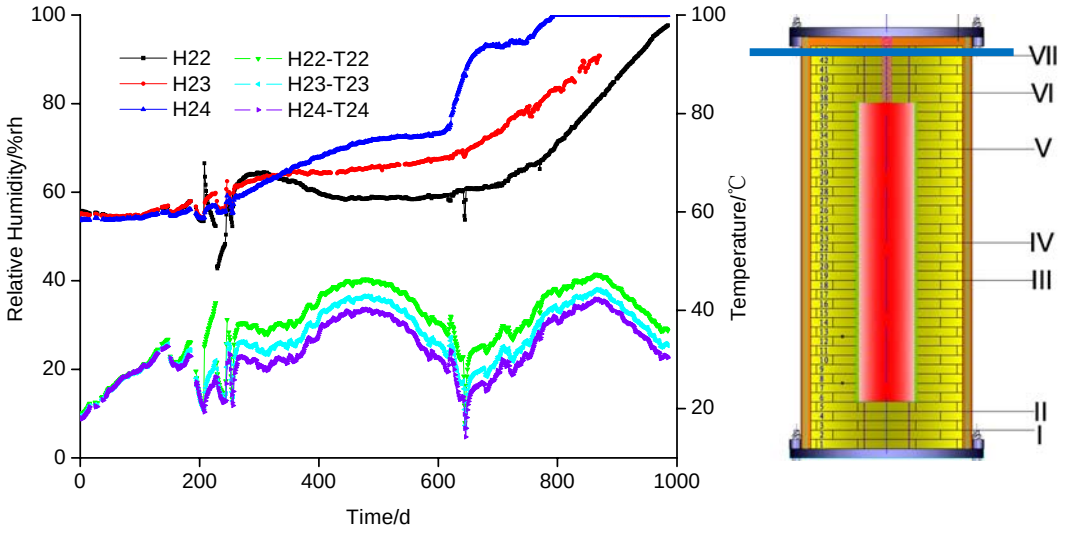

Figure 16 Variation of relative humidity with time at section VII.

3.4 Vertical displacement of the canister

In order to investigate the potential movement of canister in long-term, six LVDT sensors are installed in the China-Mock-up test to monitor the vertical displacement of the electrical heater. Three of them are installed at the bottom of the heater, and the others are installed in the upper part. The variation of the vertical displacement of the heater is presented in Fig. 17. It can be noticed that, the electrical heater moved upward after a stable phase. This phenomenon could be attributed to the thermal expansion of compacted bentonite, and the increased swelling of bentonite induced by the water penetration from outer boundary. In the proceeding of the test, the displacement became more and more flat. However, unfortunately the sensors in upper part are out of work because of the harsh environment after 800 days.

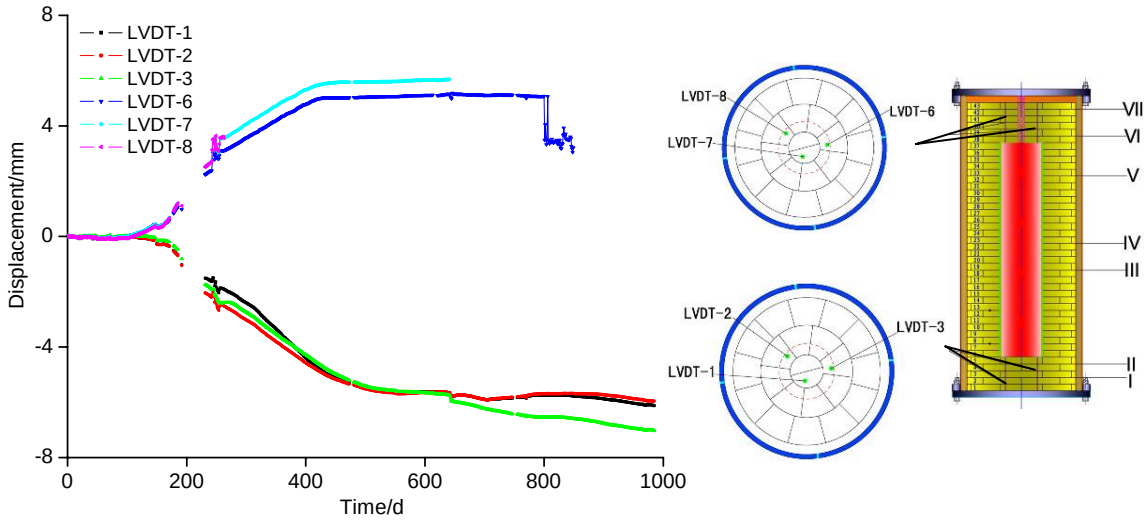

Figure 17 Vertical displacement of the heater with time.

3.5 Stress evolution

In the China-Mock-up facility, the stress variation of the compacted bentonite is influenced by several mechanisms, including the thermal expansion induced by the high temperature, the swelling pressure generated by the water penetration, and etc. The stress evolutions are presented in Fig. 18-24. As illustrated in the figures, with the increase of the injection water, the saturation process is dominant, and the stress in this area is increased gradually to 2.0Mpa especially in the outer boundary. In other sections, almost no significant variation of stress in compacted bentonite is observed up to now near the heater. This could be attributed to two reasons: at first, the saturation process is relatively limited near the heater; and the second reason is the initial space between the sensors and the blocks of the compacted bentonite. It can be noticed that there are some fluctuation in hot section III-V because of the power supply incident.

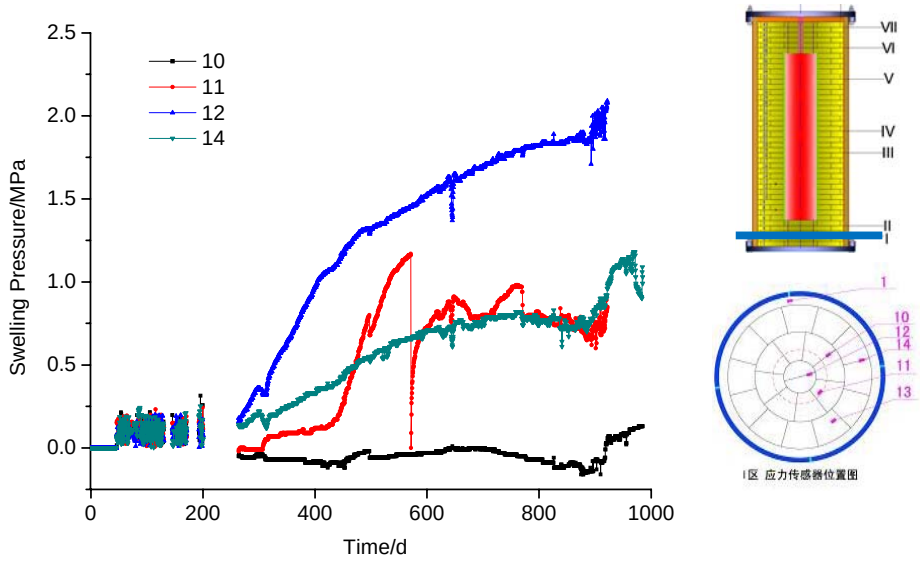

Figure 18 Stress evolution at section I of China-Mock-up.

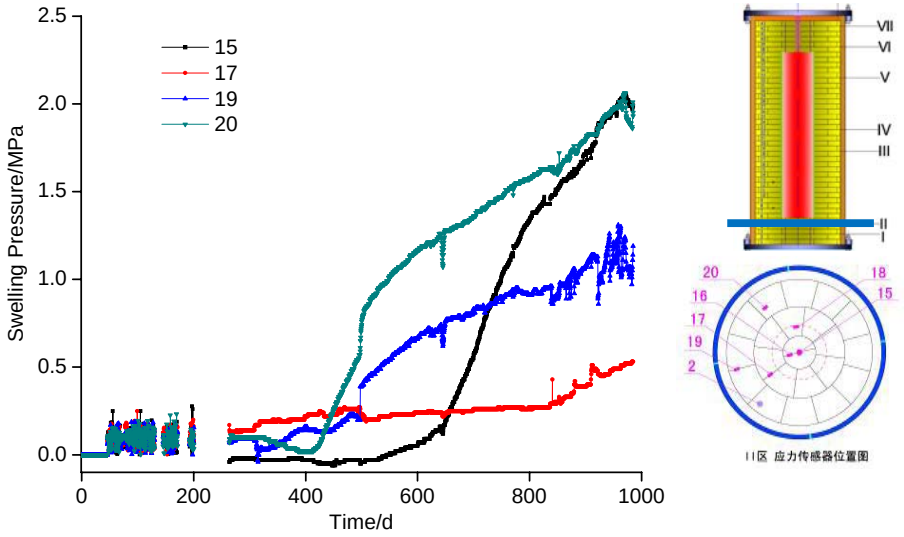

Figure 19 Stress evolution at section II.

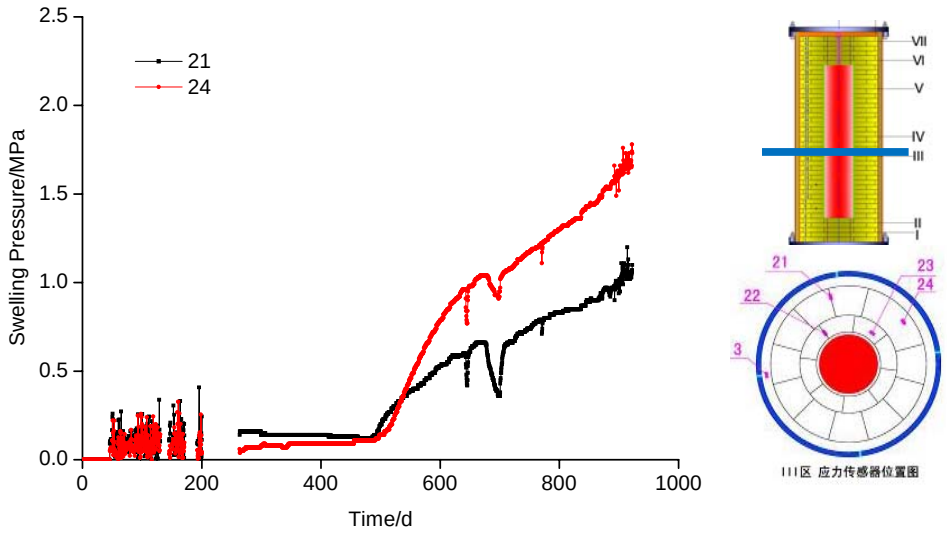

Figure 20 Stress evolution at section III.

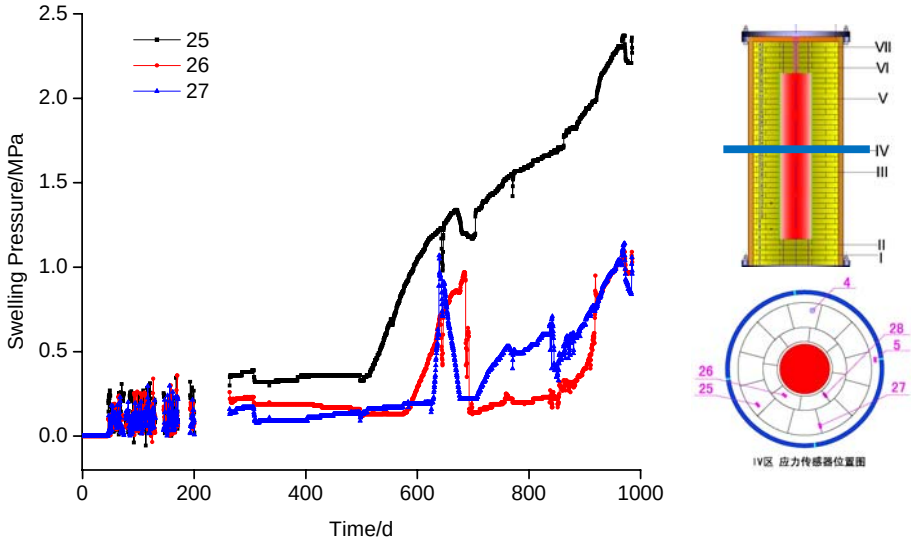

Figure 21 Stress evolution at section IV.

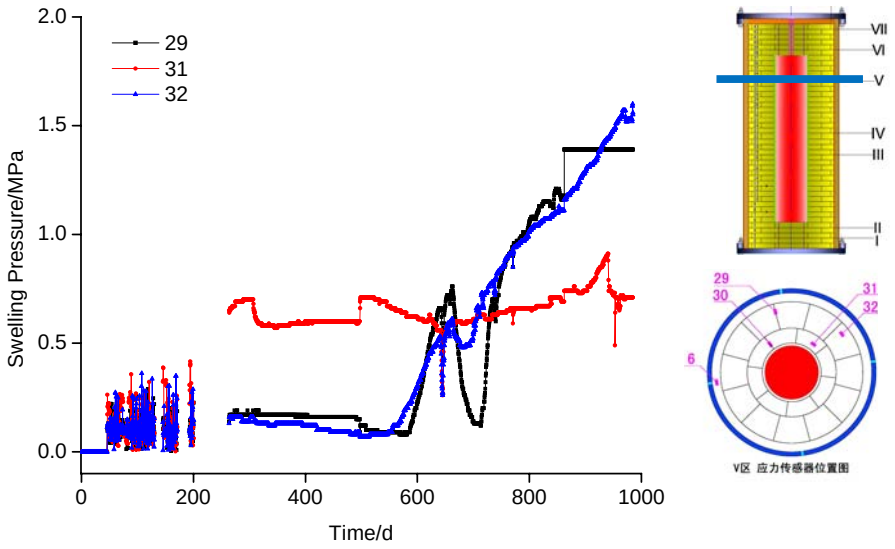

Figure 22 Stress evolution at section V.

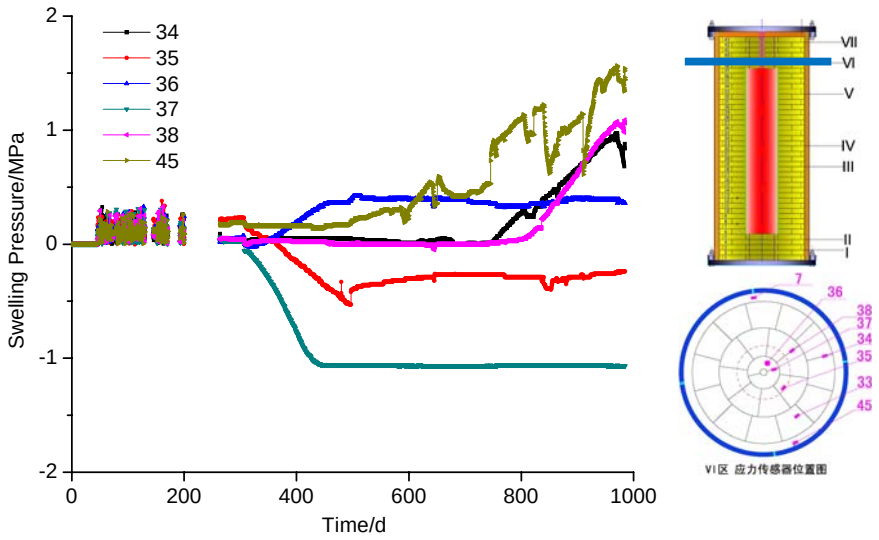

Figure 23 Stress evolution at section VI.

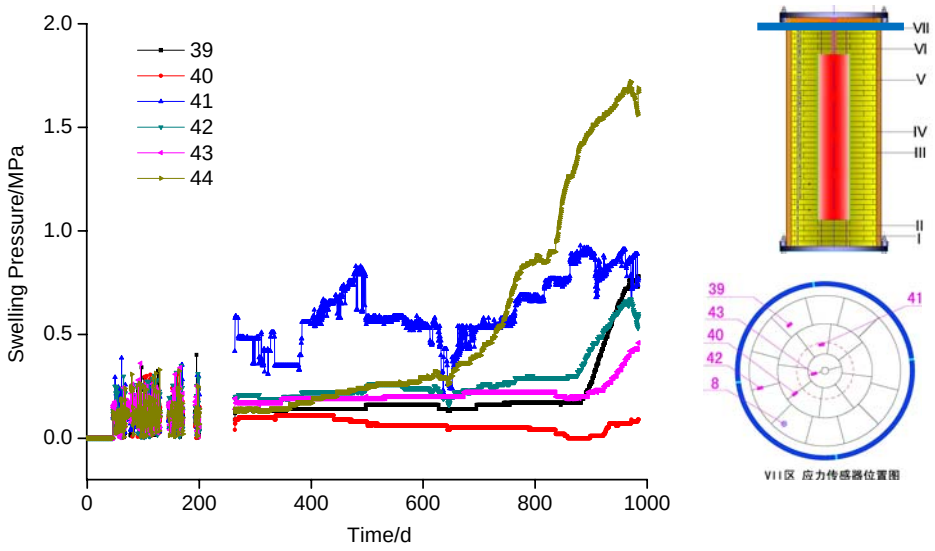

Figure 24 Stress evolution at section VII.

4. Numerical study of the China-Mock-up

4.1 constitutive model

In order to reproduce the physico-mechanical behavior of the GMZ bentonite aforementioned, a coupled THM model is proposed. In the model, various THM coupling phenomena are taken into account, including the transport of heat (conduction and convection), motion of liquid water, vapor diffusion, and their couplings with mechanical behaviors. The main formulations of the proposed model are presented in this part.

4.1.1 diffusion model

In general, the compacted bentonite is composed of three phases, namely the solid, liquid water and gas (air and water vapor). In the simulations, the conservation mass of each phase (water or gas) is assumed. The phase exchange term thus will not be considered in the balance equations. The variables chosen for the description of the flow problem are liquid water pressure, gas pressure and temperature.

(1) water species

For the water species, the mass conservation equation is obtained by summing the balance

equation of liquid water and water vapor. The equation includes the variation of water storage and the divergence of water flows in each phase. Considering water vapor is a component of gaseous phase, it thus has two contributions: the advective flux of gaseous phase and the non-advective flux of the water vapor related to vapor diffusion inside the gaseous phase, which can be written as (Collin et al., 1999):

$$\frac{\partial \rho_w n S_{r,w}}{\partial t} + \mathrm{div}(\rho_w \underline{f}_w) + \frac{\partial \rho_v n S_{r,g}}{\partial t} + \mathrm{div}(\underline{i}_v \rho_v \underline{f}_g) = 0 \quad (1)$$

where ρ_w is liquid water density; n is the medium porosity; $S_{r,w}$ is water saturation degree, $\underline{f}_\alpha$ (α=*w,g*) represents macroscopic velocity of the phase α; $\underline{i}_v$ is the non-advective flux of water vapour; ρ_v is water density; $S_{r,g}$ is the gas degree of saturation in volume and *t* is the time. ρ_v is water density; $S_{r,g}$ is the gas degree of saturation in volume and t is the time.

The generalized Darcy's law for multiphase porous medium is adopted to simulate the motion of liquid water:

$$\underline{f}_w = -\frac{k_{int} k_{r,w}}{\mu_w}[\underline{\nabla} p_w + g \rho_w \underline{\nabla} y] \quad (2)$$

where p_w is the liquid water pressure; *y* is the vertical upward directed co-ordinate; *g* is the gravity acceleration; μ_w is the dynamic viscosity of the liquid water, and k_{int} is the intrinsic permeability.

The water vapor flow is assumed to follow Fick's diffusion law in a tortuous medium. In the study, the formulation proposed by the model of Philip and Vries (1957) is adopted:

$$\underline{i}_v = -D_{atm} \tau_v n S_{r,g} \underline{\nabla} \rho_v \quad (3)$$

where D_{atm} is the molecular diffusion coefficient and τ_v is the tortuosity.

(2) Heat diffusion

In the context, one unique temperature variable is adopted. It means that the temperature is assumed to be homogenous in all phases. The heat transport is related to three effects: conduction, convection and vaporization, as presented in the following equation:

$$q' = -\Gamma \underline{\nabla} T + [c_{p,w} \rho_w \underline{f}_w + c_{p,a}(\underline{i}_a + \rho_a \underline{f}_g)] + c_{p,v}(\underline{i}_v + \rho_v \underline{f}_g)(T - T_0) + (\underline{i}_v + \rho_v \underline{f}_g) L \quad (4)$$

where Γ is the medium conductivity; $c_{p,a}$ (α=w, v, a) represents the specific heat of phase α. In general, the thermal conductivity is dependent on the temperature and saturation degree. For simplicity, the influence of temperature on thermal conductivity is not considered therein.

4.1.2 Mechanical model

Based on the experimental investigations, some constitutive models are proposed (Alonso, 1990; Alonso, 1999; Tang, 2009). The BBM model is widely used because of its capacity of representing the main fundamental features of partially saturated soils in a consistent and unified manner. It should be noted that the expensive behavior of compacted bentonite is better represented with the modified BBM model (Alonso et al., 1999) by taking into account of the microstructural variation during wetting process. However, the formulation of the model is much more complicated, and some parameters are difficult to identify. As a preliminary study, the BBM model is adopted. A brief introduction to this model is given.

(1) Yield surface

The BBM model is based on the classic Cam-clay model. In consideration of the influence of saturation degree on the mechanical behavior, suction is adopted as an independent variable in this model. The plastic yield surface is thus written in three-dimensional stress space (*p*, *q*, *s*). For the BBM model, the yield surfaces are composed of three parts. In the (*p*, *q*) space, for a given suction, the yield surface can be written as:

$$q^2 - M^2(p + p_s)(p_0 - p) = 0 \tag{5}$$

where p is the mean stress; q refers to the deviatoric stress; M is the slope of the critical line, and p_s represents the soil strength in extension.

The pre-consolidation pressure p_0 varies with the suction. The following equation is proposed which is well known as the LC curve:

$$p_0 = p_c \left(\frac{P_0^*}{p_c} \right)^{\frac{\lambda(0)-k}{\lambda(s)-k}} \tag{6}$$

where P_0^* is the pre-consolidation pressure in saturated condition; p_c is a reference pressure; k is the elastic slope of the compressibility curve against the net mean stress; $\lambda(0)$ is the plastic slope for the saturated condition, and $\lambda(s)$ refers to the plastic slope of the compressibility curve against the net mean stress (Fig. 25).

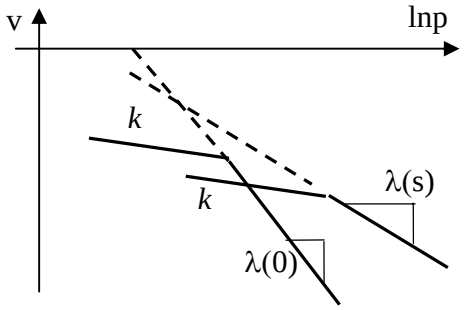

Figure 25 Compression curve for saturated and unsaturated soil.

Under unsaturated condition, the suction contributes to stiffening the soil against the external load. Hence, the plastic slope of the compressibility curve varies with the suction. The following equation is proposed to represent this phenomenon:

$$\lambda(s) = \lambda(0)[(1-r)\exp(-\beta s) + r] \tag{7}$$

where γ and β are the parameters describing the changes in soil stiffness with suction. The LC curve defines another part of the yield surface used for modeling the collapse behavior under wetting.

Numerous studies confirmed that irreversible volumetric deformation may be induced by variations in suction. Therefore, the SI yield surface, which defines the maximum previously attained value of the suction, is employed to take into account this phenomenon:

$$F_2 = s - s_0 = 0 \tag{8}$$

where s_0 represents the maximum historic suction submitted to the soil.

(2) Hardening law

The evolution of yield surfaces is assumed to be controlled by the total plastic volumetric strain ε_v^p. Two hardening laws define the evolution of state variables p_0 and s_0 with the irreversible strain:

$$\mathrm{d}p_0^* = \frac{(1+e)p_0^*}{\lambda(0)-\kappa}\mathrm{d}\varepsilon_v^p \tag{9}$$

$$\mathrm{d}s_0 = \frac{(1+e)(s_0+P_{at})}{\lambda_s - k_s}\mathrm{d}\varepsilon_v^p \tag{10}$$

where e is the porosity of the soil; P_{at} is the atmospheric pressure; λ_s and k_s are the plastic and elastic stiffness parameters for suction variation, respectively.

4.2 Determination of THM parameters

(1) Hydro-thermal properties

Among the hydro-thermal properties, the water retention curve and permeability are considered as the key factors on the water intake volume and the final saturation degree. Measured data of water content in function of suction is available (Chen et al., 2006). The relation between suction and water saturation is adopted in the study:

$$S_{r,w} = S_{r,res} + a_3 \frac{S_{r,u} - S_{r,res}}{a_3 + (a_1 s)^{a_2}} \tag{11}$$

where $S_{r,u}$ is the maximum saturation degree in the soil and $S_{r,res}$ is the residual saturation degree for a very high value of suction.

Values of $S_{r,u}$ and $S_{r,res}$ determined in test are 1.0 and 0.1, respectively. Calibration of this function on measured data gives the values of the following parameters: $a_1=3.5\times10^{-6}$ Pa^{-1}, $a_2=0.8$, $a_3=90$. Water retention curve of GMZ bentonite is illustrated in Fig. 26.

Relative permeability curves are determined based on the experimental investigation (Ye et al., 2009b), as shown in Fig. 27. The intrinsic permeability $k_{int}= 7.0\times10^{-21}$ m^2 is chosen according to the experimental data. Thus, we have

$$k_{r,w} = \frac{(S_{r,w} - S_{r,res})^4}{(S_{r,u} - S_{r,res})^4} \tag{12}$$

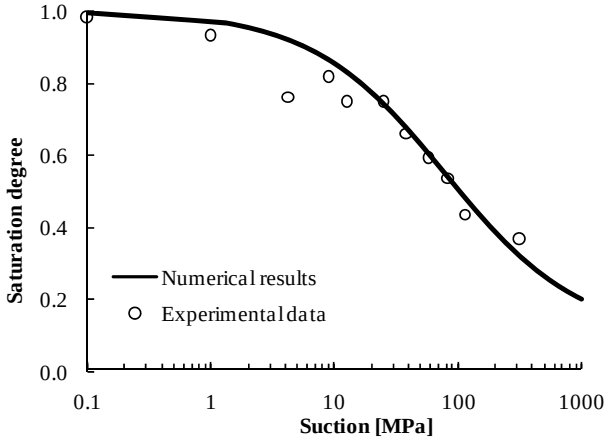

Figure 26 Water retention curve of GMZ bentonite.

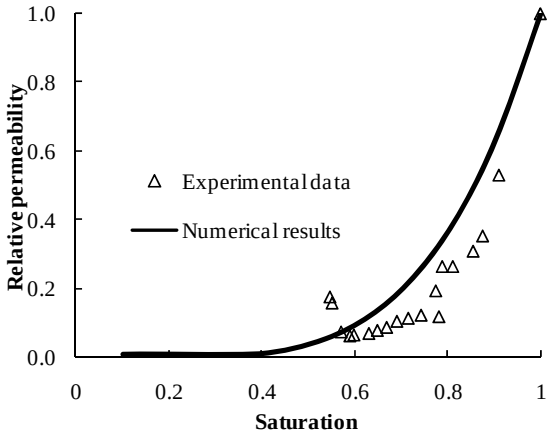

Figure 27 Variation of relative permeability in function of saturation degree.

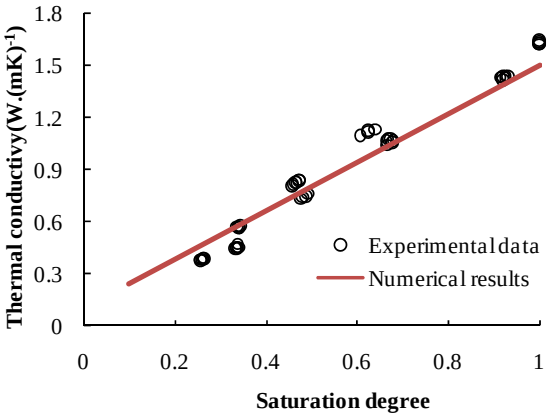

Figure 28 Variation of thermal conductivity with saturation degree.

A linear relation is adopted to describe the variation in thermal conductivity with saturation degree, as shown in Fig. 28. Table 1 summarized the other parameters of the hydraulic and thermal properties:

Table 1 Parameters of the flow model.

Grain density ρ_s (kg.m^{-3})	Grain specific heat $c_{p,s}$ (J.kg^{-1}K^{-1})	Water density ρ_w(kg.m^{-3})	Water dynamic viscosity μ_w(Pa.s)	Water specific heat $c_{p,w}$ (J.kg^{-1}K^{-1})	Air density ρ_a (kg.m^{-3})
1.6×10^{3}	2.6	1.0×10^{3}	1.009×10^{-3}	4.18×10^{3}	1.205
Air dynamic viscosity μ_a(Pa.s)	**Air specific heat $c_{p,a}$ (J.kg^{-1}K^{-1})**	**Water vapour specific heat $c_{p,v}$ (J.kg^{-1}K^{-1})**	**Latent heat of vaporization L(J.kg^{-1})**	**Tortuosity, τ**	**Intrinsic permeability, k_{int}**
1.80×10^{-5}	1.0×10^{3}	1.90×10^{3}	2.50×10^{6}	0.4	7.0×10^{-21}

(2) Mechanical parameters

The mechanical loading test at constant suction and temperature (Cui et al. 2011) revealed that elastic stiffness parameters *k* and plastic stiffness parameters λ(s) of the GMZ bentonite increase with decrease of suction but are independent of the temperature changes. The effect of temperature on the yield stress p_0 of the GMZ bentonite is found to be insignificant. For simplicity, a constant value of the elastic stiffness parameter *k* is adopted. The parameters γ and β which define the variation of $\lambda(s)$ with suction, are determined based on experimental data (Fig. 29).

The LC curve describes the evolution of p_0 with suction, which depends on *k*, λ(s) and p_c. The reference pressure p_c cannot be directly determined, thus a calibration procedure is adopted. The stiffness parameters k_s and λ_s define the volumetric strain changes induced by suction. According to the experimental study, a volumetric strain of 32.4% is obtained when the suction is decreased from 110 to 9 MPa. Considering that the volumetric strain is induced in a wetting procedure (inferior to the maximum historic suction), it can be considered as elastic volumetric strain. Therefore, a value of 0.08 is determined for k_s. Due to the lack of experimental data, an average value of λ_s obtained from other types of Bentonite (0.25) is taken in the simulation (Collin et al., 1999). Based on the water retention curve, s_0 can be fixed from the initial saturation degree.

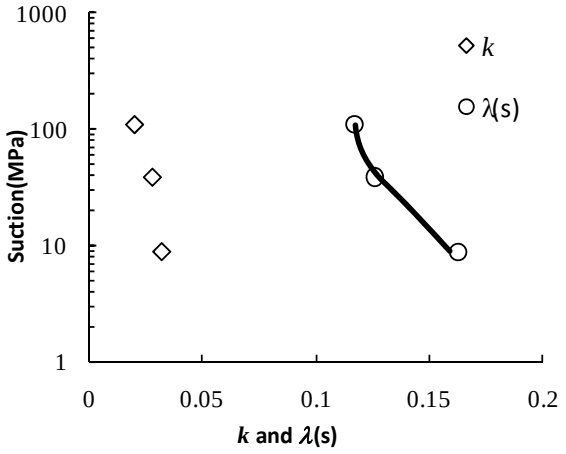

Figure 29 Variation of k and λ(s) with suction.

The dependence of these parameters on the stress state generated in the soil sample is not

taken into account. The values of parameters used in the simulations are summarized in Table 2.

Table 2 Parameters employed in mechanical model.

Saturated virgin compression index $\lambda(0)$	Elastic compression index k	Saturated pre-consolidation pressure p^*_0 (MPa)	Elastic stiffness index upon suction k_s	Plastic stiffness index upon suction λ_s	Maximum value of the suction s_0 (MPa)
0.18	0.027	0.6	0.08	0.25	80

Reference stress p_c (MPa)	Ratio $\lambda(s)/\lambda(0)$ for high suction γ	Parameters to control the increase of stiffness with suction β (MPa^{-1})
0.45	0.65	0.045

4.3 Numerical simulations

In order to validate the proposed, the numerical simulations of the China-Mock-up test are carried out with the given parameters.

4.3.1 Thermal simulation

1) Geometry and Boundary Conditions

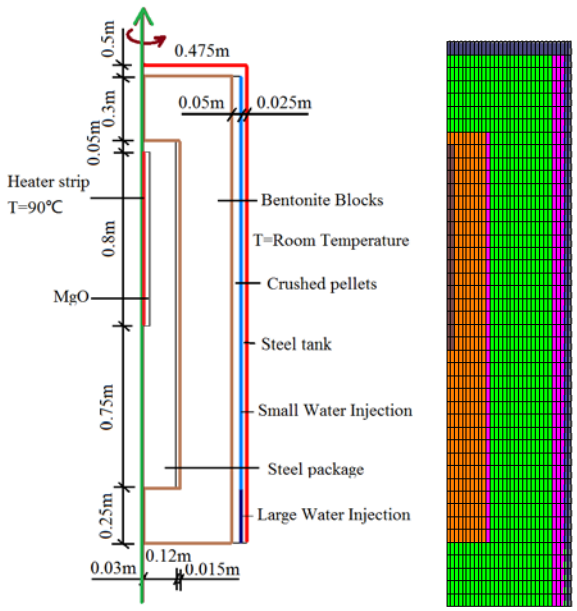

Figure 30 Boundary conditions and mesh.

An improved 2D-axisymetric finite element simulation is realized with the help of the software LAGAMINE. It has been applied to carry out the quantitative numerical study of

temperature. There are three components in the model and all the components are set to THM elements: electrical heater, GMZ bentonite and steel tank (contains the thermal insulation material). The geometry and boundary conditions are illustrated in Fig. 30.

The steel tank is neglected to address the problem in the numerical test. The fixed horizontal/vertical displacement is imposed on the nodes around the perimeter. The constant temperature is imposed on the nodes of the electrical heater and on the nodes in contact with the atmosphere. The hydration influence is modeled by increasing water injection on the nodes of bentonite's outer boundary. The convection transfer between the steel tank and the atmosphere is simulated thanks to frontier thermal elements. In the simulations, air flow is not considered, whereas the vapor diffusion is assumed.

The system is initially at temperature of 0 °C. The gas pressure is assumed to be constant in order to have a better numerical convergence. The compacted GMZ bentonite has an initial water saturation of 48% and a void ratio of 0.57. According to the water retention curve determined, a suction of 80MPa is initially employed. As aforementioned, the dissolved air will not be taken into account.

Following the experimental procedure, the numerical simulations are divided into two phrases: the temperature on the nodes of the electrical heater and the water injection on the bentonite's outer boundary are increased to 90℃ and 1200g/day. The temperature on the outer boundary changes according to actual room temperature. The two temperature boundary conditions are illustrated in Fig. 31 and Fig. 32.

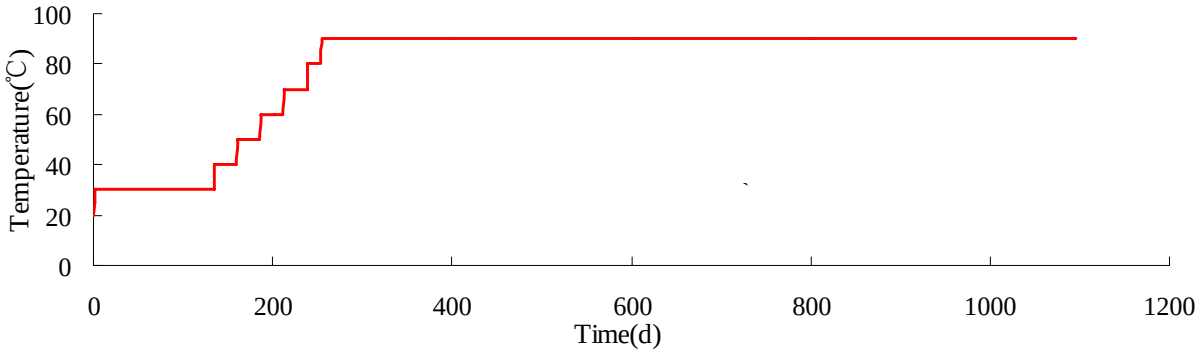

Figure 31 Heating process of the electrical heater

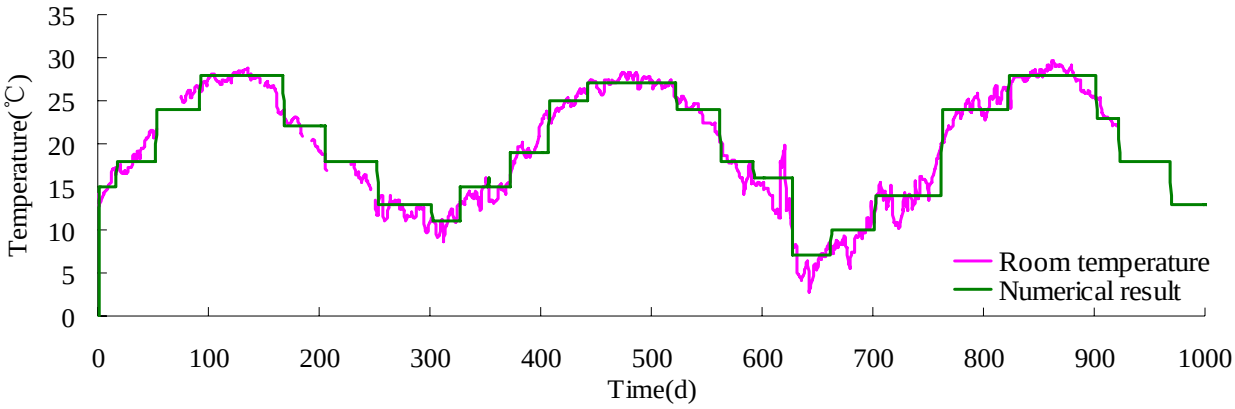

Figure 32 Temperature variation trend of the room temperature boundary

2) Quantitative analysis and results

The simulated temperature with time is illustrated in Fig.33. In the first few months, the temperature of the compacted bentonite increases significantly. Afterwards the high temperature area expands slowly. It can be noticed that the temperature of the steel elements remains in a low level, mainly as a result of the low thermal conductivity of the heat insulating material outside the steel tank.

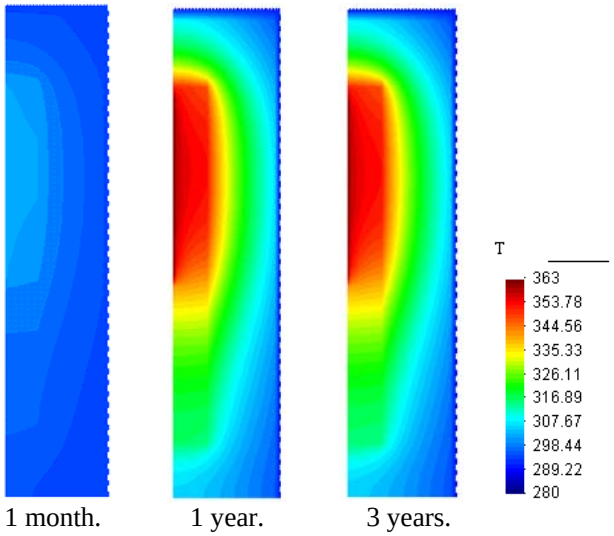

Figure 33 Distribution of temperature

The temperature variation with time of the lower part in China-Mock-up is illustrated in Fig.34. Numerical simulation results indicate the model used in the calculation has rationality.

It can also be noticed that the simulation results are greatly fluctuated due to the effect of room temperature.

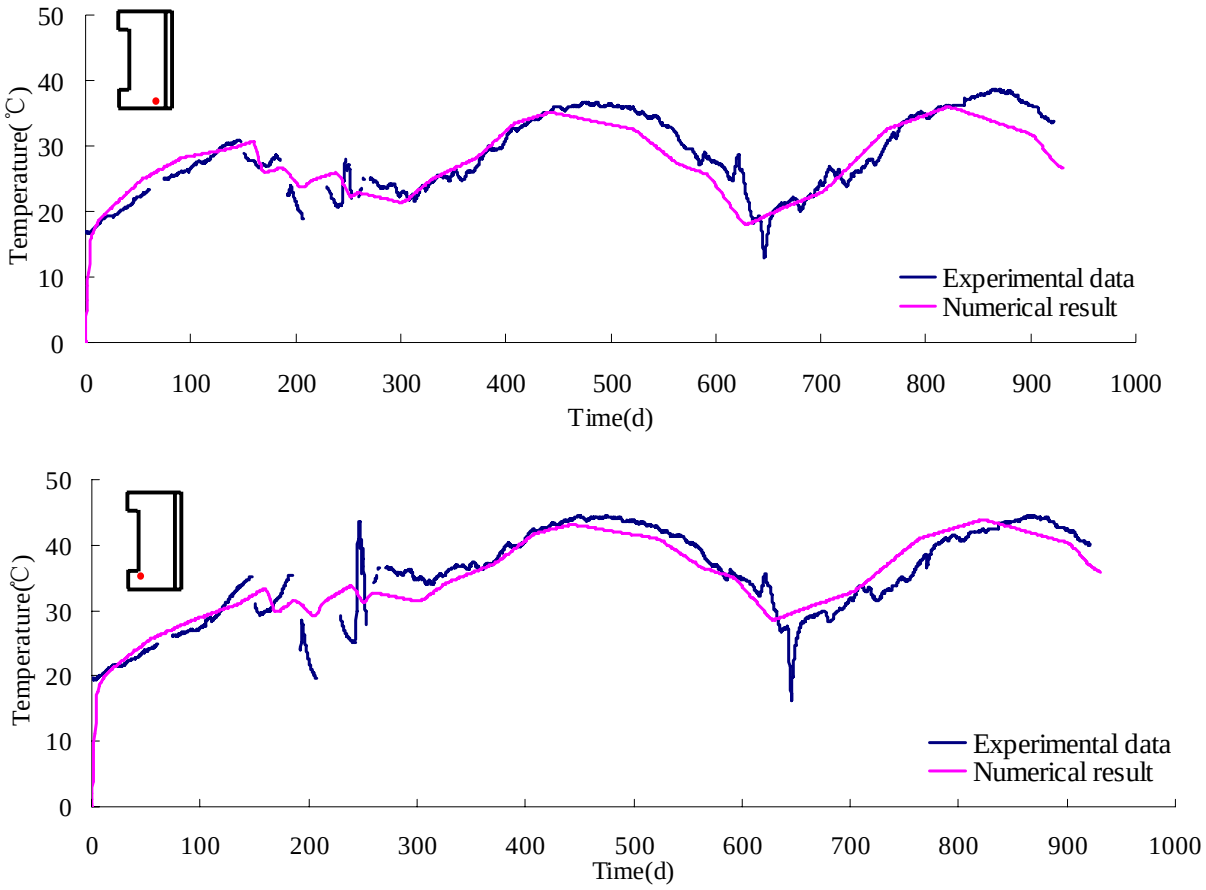

Figure 34 Temperature variation of the bottom in China-Mock-up

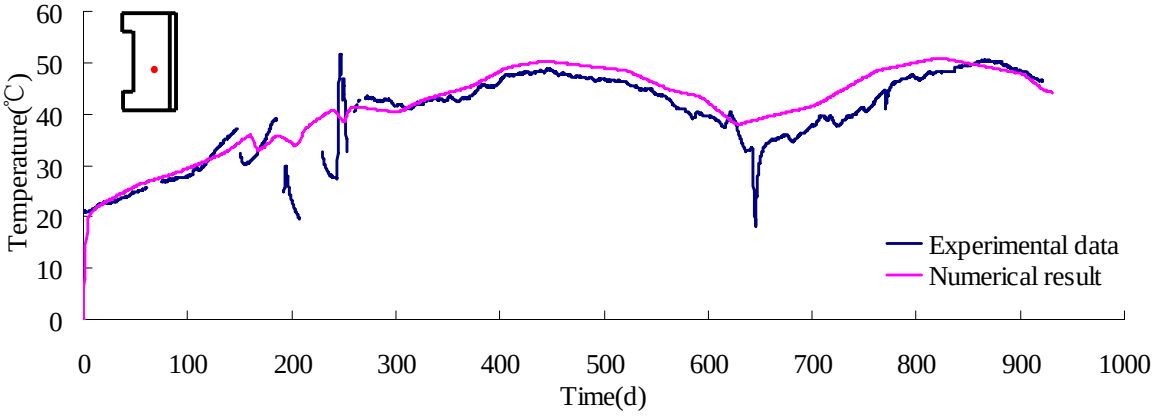

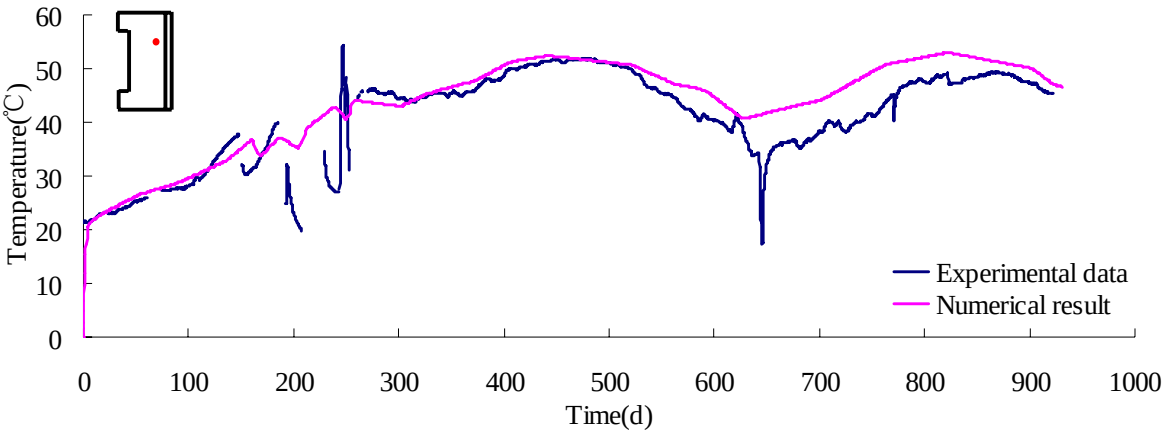

Figure 35 Temperature variation of the mid area in China-Mock-up

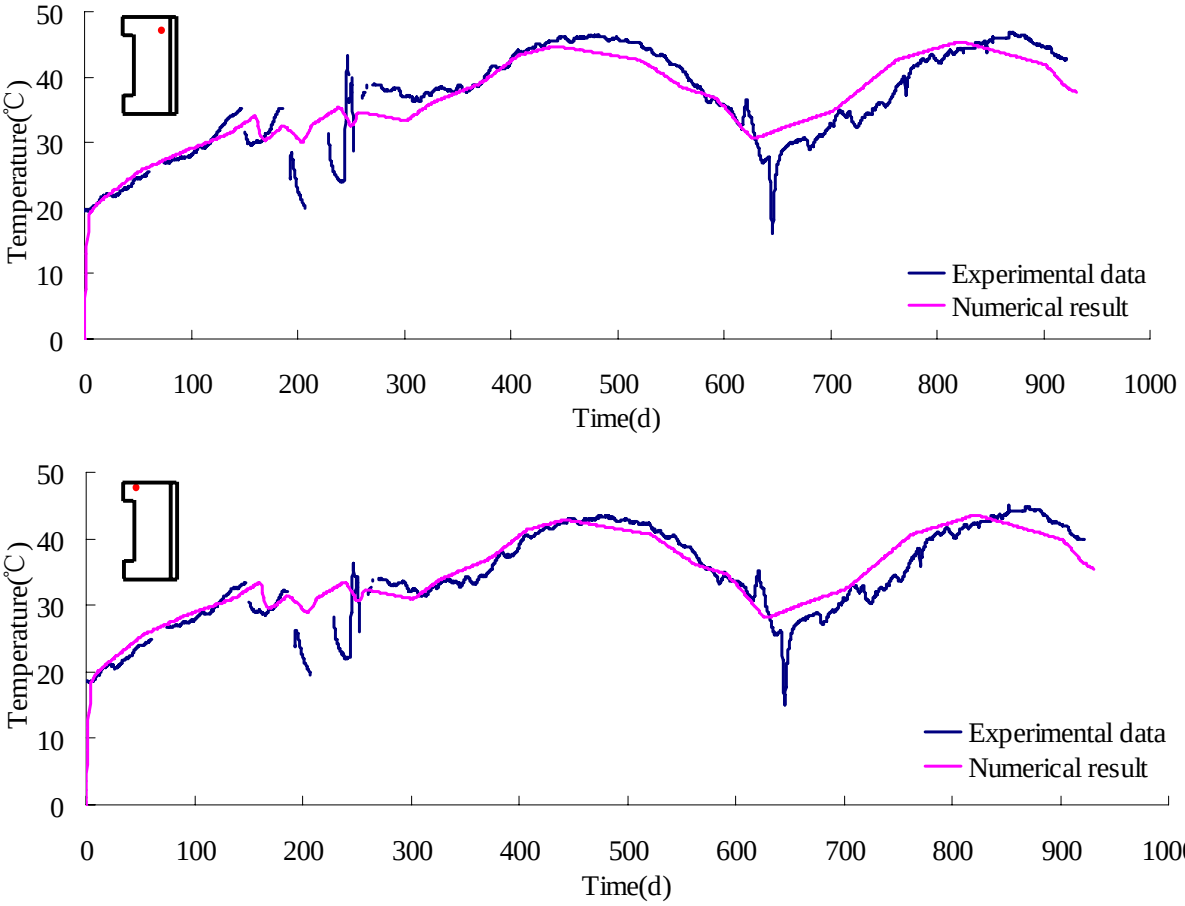

Figure 36 Temperature variation of the upper area in China-Mock-up

The temperature variations with time at some other points in GMZ bentonite are shown in

Fig 35 and Fig 36. As mentioned, the temperature of the bentonite grow rapidly in the first year and then to stabilize. It can also be noticed that the points closer to the heater are less affected by room temperature.

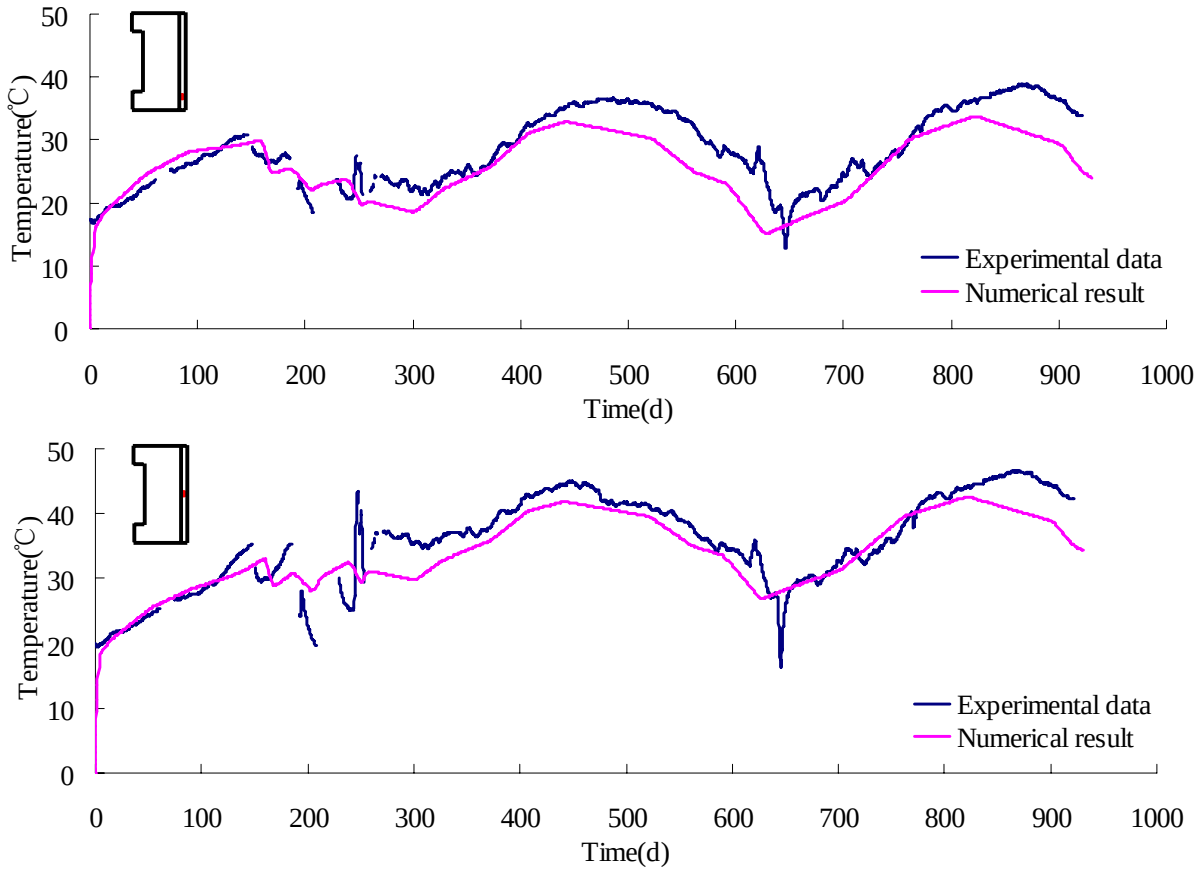

Figure 37 Temperature variation of the crushed pellets in China-Mock-up

Thanks to the frontier thermal elements, the temperature of the crushed pellets also changes with time. Its numerical results are illustrated in Fig.37. It's clear to see that the simulation result is slightly lower than the experimental data. It indicates that room temperature variation plays a major role to crushed pellets in the simulation.

4.3.2 Hydro-thermal simulation

1) Geometry and Boundary Conditions

When it comes to Hydro-thermal simulations, there will be some convergence problems if using the model as illustrated in Fig. 30. Therefore a simplified model is tentatively used to

carry out the Hydro-thermal simulations. The water injection on the boundary is different as the lower part has a lager water injection. The geometry and boundary conditions are illustrated in Fig. 38.

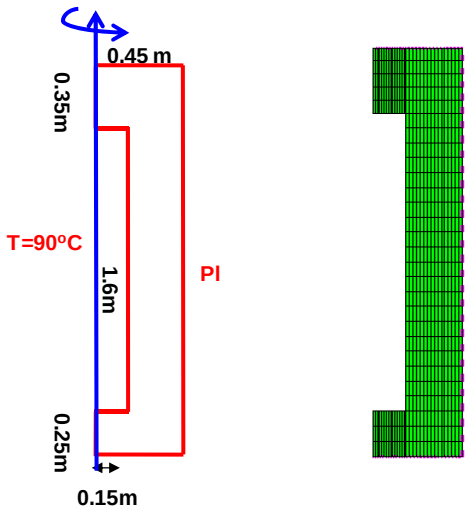

Figure 38 Boundary conditions and mesh

For simplicity, the steel tank is neglected to address the problem in the numerical test. The fixed horizontal/vertical displacement is imposed on the nodes in contact with the steel. The heating is simulated by imposing the temperature on the nodes in contact with the heater and the steel tank. The hydration influence is modeled by increasing water pressure on the nodes of outer boundary. The convection transfer between the GMZ bentonite and atmosphere is simulated thanks to frontier thermal elements. Similarly, air flow is not considered in the simulations, whereas the vapor diffusion is assumed. The initial state and the boundary conditions are same as the thermal simulation.

2) Quantitative analysis and results

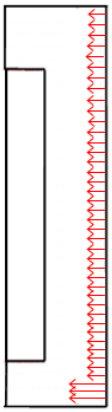

Figure 39 Water flow during the simulation

The compacted bentonite is progressively saturated by the water inflow, which is in an opposite direction to heat flow. However, due to the extremely low permeability and evaporation, the compacted bentonite close to the heater still stays partially saturated after 3 years (Fig. 39).

The numerical calculation of water pressure with time is illustrated in Fig.40. As a result of the different water injection on the boundary, the water pressure of the bottom is higher than the other areas. It is noticed that in the field exposed to high temperature, the water pressure decreases over time. This result seems reasonable considering that the evaporation generated by high temperature is more significant in this area.

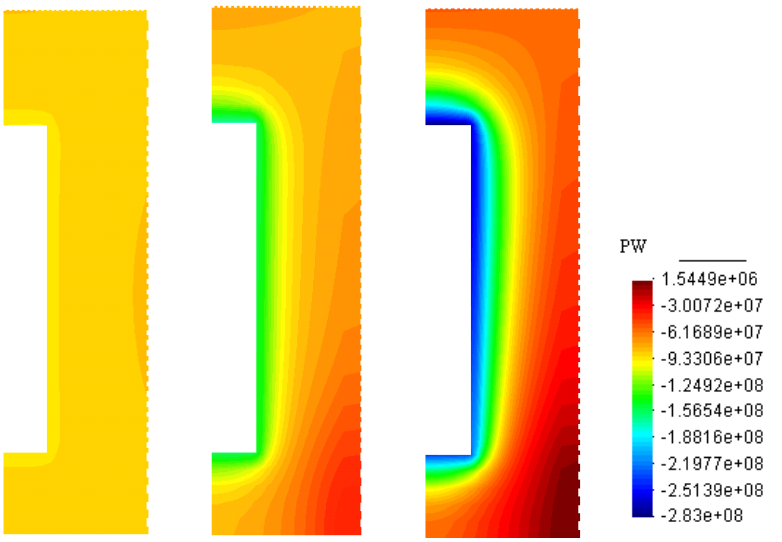

Figure 40 Distribution of water pressure

Numerical results of relative humidity at some points in China-Mock-up are illustrated in Fig.41 and Fig.42. It is interesting that the saturation of the internal bentonite is firstly increased and then decreased. This can be explained by active vapor diffusion under the effect of high temperature. In contrast, the relative humidity of the area that far from the heater continues to increase over time. It indicates that the hydraulic effect is more significant in these areas.

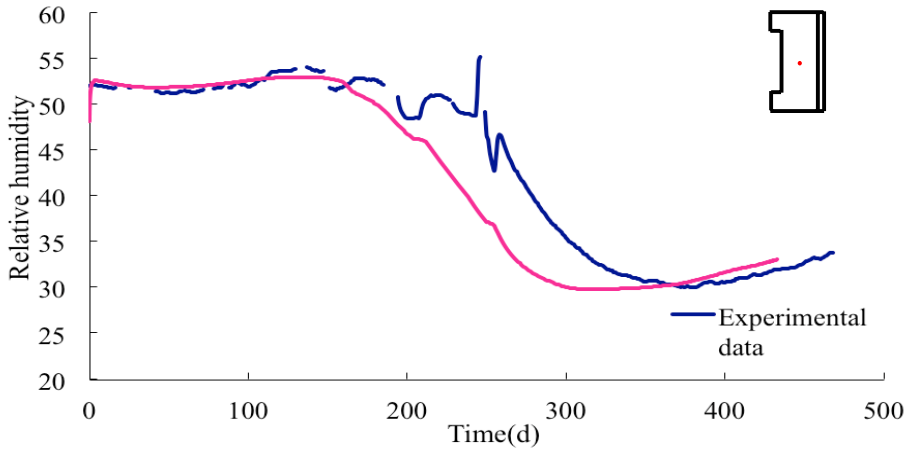

Figure 41 Numerical result of relative humidity at a point in China-Mock-up

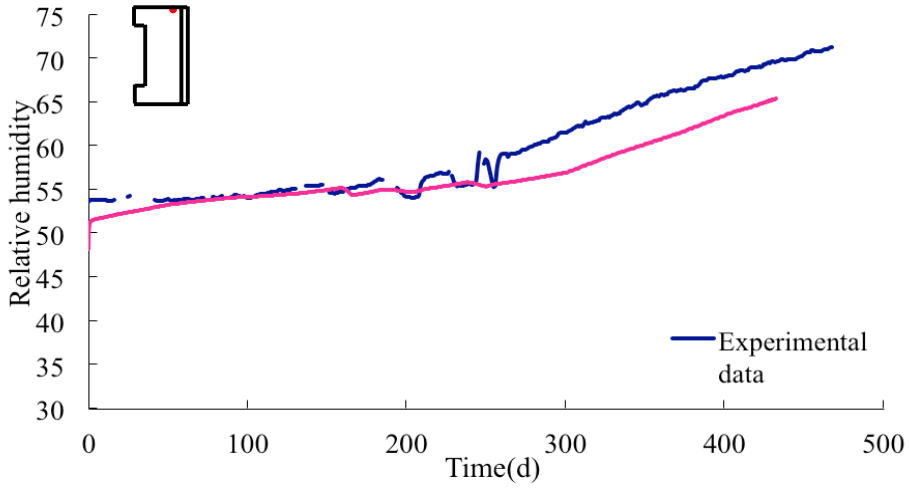

Figure 42 Numerical result of relative humidity at a point in China-Mock-up

5. Conclusion

The buffer material is one of the main engineered barriers for the HLW repository. In order to study the behavior of the compacted GMZ-Na-bentonite under coupled THMC conditions, a

large-scale mock-up facility, China-Mock-up based on a preliminary concept of HLW repository in China, has been designed and constructed in the laboratory of BRIUG.

The current experimental data is presented in the report, including the variation of temperature, relative humidity, stress and displacement etc. A thermo-hydro-mechanical model is proposed to reproduce the complex coupling behavior of the compacted GMZ bentonite. With the proposed model, numerical simulation of the China-mock-up test is realized. According to the analysis of the experimental and numerical results, some conclusions are obtained and summarized as follows:

(1) The experimental data indicates that the saturation process of the compacted bentonite is strongly influenced by the competitive mechanism between the drying effect induced by the high temperature and the wetting effect by the water penetration from the outer boundary. For this reason, the desiccation phenomenon is observed in the zone close to the heater.

(2) Except for the temperature change induced by the interruption of electrical power supply, the temperature within the bentonite has increased with time. Considering the saturation may change the thermal conductivity, the temperature distribution is influenced by the coupling mechanism between the thermal conduction and the saturation process in the mock-up test. However, it is noticed that the change of seasons has a significant effect on temperature.

(3) For China-mock-up test the upward displacement of the heater suggests that the thermal expansion and saturation process of the buffer material may influence the stability of canister in the long-term, which should be considered in the design of the repository. It has to be mentioned here, the displacement of electrical heater is strongly influenced by the experimental configuration and boundary conditions. Considering the repository conception in China is not finalized yet, the similar weight of the canister and electrical heater cannot be assumed. Therefore, this result is not totally representative of the real ones, and further validation is still necessary.

(4) In the China-Mock-up facility, the stress variation of the compacted bentonite is influenced by several mechanisms, including the thermal expansion induced by the high temperature, the swelling pressure generated by the water penetration, and etc.

(5) Based on the quantitative analysis of the numerical results, it is suggested that the proposed model is capable to reproduce the principal thermal behavior of the compacted

GMZ bentonite. As a quantitative analysis of the numerical results, the numerical study for now can be considered as a preliminary stage. With the progress of the experimental test, further quantitative studies are needed.

The China-Mock-Up experiment is an important milestone of the buffer material study for HLW disposal in China. The observed THMC processes taking place in the compacted bentonite-buffer during the early phase of HLW disposal can provide a reliable database for numerical modeling and further investigations of EBS, and the design of HLW repository.

6. References

Akesson M, Borgesson L, Kristensson O., 2010. THM modeling of buffer, backfill and other system components: critical processes and scenarios. Stockholm: SKB technical report.

Alonso E E, Gens A, Josa A., 1990. A constitutive model for partially saturated soils. Géotechnique, 40 (3): 405–430.

Alonso E E, Vaunat J, Gens A., 1999. Modelling the mechanical behavior of expansive clays. Engineering Geology, 54 (1): 173–183.

Chen, B., Qian, L.X., Ye, W.M., Cui, Y.J. & Wang, J. 2006. Soil-water characteristic curves of Gaomiaozi bentonite. *Chinese Journal of Rock Mechanics and Engineering*, 25 (4): 1054-1058.

Charlier R., 1987. Approach unifiée de quelques problèmes non linéqires de mécanique des milieux continus par la méthode des éléments finis. Ph.D. Thesis. Liège: Université de Liège.

Collin F, Li X L, Radu J P, Charlier R. 1999. Thermo-hydro-mechanical coupling in clay barriers. Engineering Geology, 54 (2/3): 173–183.

Cui Y J, Tang A, Quian L X, Ye W M, Chen B., 2011. Thermal-mechanical behavior of Compacted GMZ bentonite. Soils and Foundations, 51 (6): 1065–1074.

Chen L., Wang J., Liu Y.M., et al., 2012. Numerical thermo-hydro-mechanical modeling of compacted bentonite in China-mock-up test for deep geological disposal. Journal of Rock Mechanics and Geotechnical Engineering, 2012, 4(2): 183-192.

Gens, A., Guimarães, L. do N., Olivella, S. & Sánchez, M. 2010. Modelling thermo-hydro-mechano-chemical interactions for nuclear waste disposal. *Journal of Rock Mechanics and Geotechnical Engineering*. 2010, 2 (2): 97-102.

Karnland, O., Sandén T., Johannesson Lars-Erik, et al. 2000. *Long term experiment of buffer material, Final report on the pilot parcels*, SKB Technical Report, TR-00-22.

Li, X. L., Frédéric, B & Johan, B. 2006. The Belgian HLW repository design and associated R&D on the THM behaviour of the host rock and EBS. *Chinese Journal of Rock Mechanics and Engineering*, 2006, 25 (4): 682-692.

Li, X. L., Bastiaens, P., VanMarcke, P, et al. 2010. Design and development of large-scale in-situ PRACLAY heater experiment and horizontal high-level radioactive waste disposal gallery seal experiment in Belgian HADES. *Journal of Rock Mechanics and Geotechnical Engineering*. 2010, 2 (2): 103–110.

Lloret, A. & Villar, M.V. 2007. Advances on the knowledge of the thermo-hydro-mechanical behaviour of heavily compacted "FEBEX" bentonite. *Physics and Chemistry of the Earth*. 2007, 32: 701-715.

Liu, Y.M., Wen, Z.J., 2003. Study on clay-based materials for the repository of high level radioactive waste. *Journal of Mineralogy And Petrology*, 2003, 23(4): 42-45. (in Chinese)

Liu, Y.M., Cai M.F., Wang J., 2007a. Compressibility of buffer material for HLW disposal in China. *Uranium Geology*, 23, 91-95. (in Chinese)

Liu, Y.M.,Wang, J.,Zhao, X.G., et al. 2011. Design and development of a large-scale THMC experiment of compacted bentonite for geological disposal of high level radioactive waste in China. Proceeding of the 12th ISRM international congress on rock mechanics, Beijing, China, 2011, 556-557.

Pacovsky J., Svoboda J. & Zapletal L., 2007. Saturation development in the bentonite barrier of the Mock-Up-CZ geotechnical experiment. *Physics and Chemistry of the Earth*, 32(2007), 767-779.

Philip J R, de Vries D A. 1957.Moisture movement in porous materials under temperature gradients. Transactions, American Geophysical Union, , 38 (2): 222–232.

Romero, E., Li, X. L. 2006. Thermo-hydro-mechanical characterization of OPHELIE backfill mixture. *Chinese Journal of Rock Mechanics and Engineering*, 2006, 25 (4): 733-740.

Tang A M, Cui Y J., 2009. Modelling the thermo-mechanical volume change behaviour of compacted expansive clays. Geotechnique, 59 (3): 185–195.

Wang, J. 2010. High-level radioactive waste disposal in China: update 2010. *Journal of Rock Mechanics and Geotechnical Engineering*, 2010, 2 (1): 1–11.

Ye, W.M., Cui, Y.J., Qian L.X. & Chen, B., 2009a. An experimental study of the water transfer through confined compacted GMZ-bentonite. *Engineering Geology*, 108(3-4): 169-176.